**Structural Engineering and Mechanics**, *Vol. 78, No. 5 (2021) 623-635*
DOI: https://doi.org/10.12989/sem.2021.78.5.623


# Seismic performance of exterior R/C beam-column joint under varying axial force

Yanbing Hu*[1], Masaki Maeda[1a], Yusuke Suzuki[2b] and Kiwoong Jin[3c]

[1]*Graduate School of Engineering, Tohoku University, Sendai, Japan*
[2]*Graduate School of Engineering, Osaka City University, Osaka, Japan*
[3]*Graduate School of Science and Technology, Meiji University, Kawasaki, Japan*

(*Received November 13, 2018, Revised December 13, 2020, Accepted May 3, 2021*)

**Abstract.** Previous studies have suggested the maximum experimental story shear force of beam-column joint frame does not reach its theoretical value due to beam-column joint failure when the column-to-beam moment capacity ratio was close to 1.0. It was also pointed out that under a certain amount of axial force, an axial collapse and a sudden decrease of lateral load-carrying capacity may occur at the joint. Although increasing joint transverse reinforcement could improve the lateral load-carrying capacity and axial load-carrying capacity of beam-column joint frame, the conditions considering varying axial force were still not well investigated. For this purpose, 7 full-scale specimens with no-axial force and 14 half-scale specimens with varying axial force are designed and subjected to static loading tests. Comparing the experimental results of the two types of specimens, it has indicated that introducing the varying axial force leads to a reduction of the required joint transverse reinforcement ratio which can avoid the beam-column joint failure. For specimens with varying axial force, to prevent beam-column joint failure and axial collapse, the lower limit of joint transverse reinforcement ratio is acquired when given a column-to-beam moment capacity ratio.

**Keywords:** exterior beam-column joint; column-to-beam moment capacity ratio; axial force; joint transverse reinforcement ratio; joint failure; axial collapse

## 1. Introduction

In the reinforcement concrete moment resisting frame, the beam-column joint plays a vital role in preventing severe building collapse against earthquakes. To avoid the beam-column joint failure, a weak beam-strong column system is requested in most international codes (ACI 318M-02, NZS 3101 2006, EC8 2003). As Uma *et al*. (2006) concluded that there are specified design factors and the relevant expressions for beam-column joint in all the codes which require the flexural strength of column be more than that of the adjoining beams to ensure beam yield mechanism.

Recently, the use of longitudinal reinforcing bars with high strength or large diameter in a relatively smaller column section, sometimes preferred in the design of buildings, causes high stress in the beam-column connections (Shiohara 2001). To predict the strength and failure type of beam-column joints, Shiohara (2004) presented a new concept of quadruple flexural resistance in RC beam-column joints which can be applied to interior, exterior and knee joints. Through the recent studies, it was found that an increase of the joint transverse reinforcement can focus the damage on beam and improve the strength of beam-column joint frame to a certain extent (Shiohara 2010, Sung 2014, Kim 2015). However, experimental results revealed that due to the joint failure, the maximum experimental story shear force of joint frame did not reach its theoretical value when the column-to-beam moment capacity ratio was close to 1.0 (Shiohara 2012). To define the reduction degree between the maximum experimental story shear force and its theoretical value, Kusuhara *et al* (2010) proposed formulae to predict the actual value of ultimate story shear force and assumed failure mechanism based on a nine DOF (degree of freedom) model. Shiohara (2014) proposed simplified equations predicting ultimate strength of RC beam column joints failed in joint hinging mechanism.

Meanwhile, many studies on the beam-column joint under axial force had been conducted. By testing 8 one-third scale specimens consisting of four pairs of interior and exterior beam-column, Fujii *et al.* (1991) found that with the increase of column axial load level, the maximum experimental story shear force was obviously improved. Fu *et al*. (2000) verified it favorable to improve the energy dissipation capacity of joints due to the increase of axial load ratio. Hwang *et al*. (2004), Yoshimura *et al*. (2004) proved that with the increase of axial load ratio, the increase in strength and ductility was observed, though the axial collapse would be more likely to happen.

Several authors also studied the behavior of an isolated

*Corresponding author, Master Student
E-mail: huyanbing199@gmail.com
[a]Professor
E-mail: maeda@rcl.archi.tohoku.ac.jp
[b]Lecturer
E-mail: ysuzuki@arch.eng.osaka-cu.ac.jp
[c]Lecturer
E-mail: jin@meiji.ac.jp



ISSN: 1225-4568 (Print), 1598-6217 (Online)

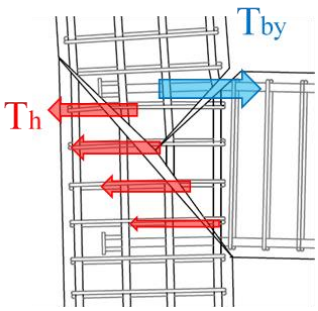


Fig. 1 Definition of transverse reinforcement ratio

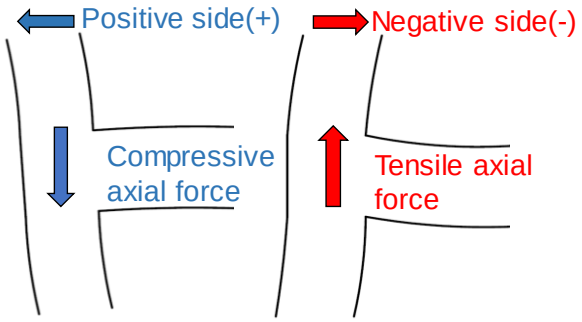


Fig. 2 Varying axial force

column subjected to axial load analytically and experimentally. A non-symmetrical characteristic was observed in the columns subjected to the varying axial force (Li 1988). Elwood *et al.* (2005) introduced a model to estimate the axial capacity of a column which had previously experienced a shear failure. By testing eight full-scale RC columns with ties of large spacing, Henkhaus *et al.* (2013) quantified the effect of transverse reinforcement at the column on the capacity of columns to deform laterally after shear failure. Tran *et al.* (2018) evaluated the story shear force and the drift ratio of axial failure through tests of short columns with limited transverse reinforcement.

In this paper, static loading tests of 7 full-scale specimens with non-axial force and 14 half-scale specimens with varying axial force are experimentally investigated. The hysteretic curves and damage situations of two types of specimens have been compared. Through the analysis of story shear force and deformation situation of specimens, it has been proved that introducing the varying axial force leads to a decrease of the required joint transverse reinforcement ratio. The lower limit of joint transverse reinforcement ratio to avoid the beam-column joint failure and the axial collapse has been discussed. In addition, the simplified equation $\beta_j$ of AIJ Standard for Lateral Load-carrying Capacity Calculation (2016) that predicting the lateral load-carrying capacity of exterior concrete beam-column joint has been verified.

## 2. Experimental outline

### *2.1 Specimen design*

In this study, specimens are considered as an exterior column-beam joint on the lower story of a reinforced concrete high-rise building. Column-to-beam moment capacity ratio, joint transverse reinforcement ratio and varying axial ratio are parameters. The column-to-beam moment capacity ratio is defined as the follows

$$R = \frac{M_{cu1} + M_{cu2}}{M_{bu}} \tag{1}$$

where $R$ is the column-to-beam moment capacity ratio, $M_{cu1,2}$ are the ultimate nodal bending moments of the upper and lower columns respectively, $M_{bu}$ is the ultimate nodal bending moments of the beam.

As illustrated in Fig. 1, the deformation is assumed to happen in the joint panel subjected to the seismic force. The joint transverse reinforcement ratio ($T_h/T_{by}$) is calculated as follows

$$\frac{T_h}{T_{by}} = \frac{\sum A_{jw} f_{jy}}{\sum A_t f_y} \tag{2}$$

where $\Sigma A_{jw}$ is the total section area of beam longitudinal reinforcement bars on the tension side, $f_{jy}$ is the yield point of beam longitudinal steel bars, $\Sigma A_t$ is the total section area of the joint transverse reinforcement bars, $f_y$ is the yield point of transverse reinforcement bars.

As illustrated in Fig. 2, varying axial force ratio is divided into compressive axial force ratio ($\rho_C$) and tensile axial force ratio ($\rho_T$).

$$\rho_C = \frac{N + Q_b}{b \cdot D_c \cdot F_c} \tag{3}$$

$$\rho_T = \frac{N + Q_b}{\Sigma at \cdot f_{cy}} \tag{4}$$

where $N$ is the axial force loaded on the upper of column, $Q_b$ is the beam shear force, $b$ is the width of column section, $D_c$ is the depth of column section, $F_c$ is the strength of concrete, $\Sigma a_t$ is the total section area of longitudinal reinforcement bars at the column, $f_{cy}$ is the yield point of column longitudinal steel bars.

The parameters are calculated according to the results of material tests. The main parameters are decided by the rules as follows:

Based on the previous researches (Shiohara 2010, 2012), the column-to-beam moment capacity ratios are set to be approximately 1.2 and 1.5. The joint transverse reinforcement ratios are designed to be at the range of 0.15-0.72. When the joint transverse reinforcement ratio is 0.15, it is slightly larger than the lower limit of AIJ Standard for Structural Calculation of Reinforced Concrete Structures (2010). The varying axial force ratios are defined according to the investigated data of real buildings subjected to seismic force. The compressive axial force ratios are set at the range of 0.18-0.47, while the tensile axial force ratio of specimens with varying axial force is set to be approximately -0.60.

The designation for naming each specimen is decided by the values of the test parameters. For instance, in T15-30T6C4, the first T represents the shape of the exterior

Table 1 List of specimens with non-axial force

| Test specimen | | T15-70 | T15-40 | T15-15 | T12-70 | T12-60 | T12-50 | T12-40 |
|---|---|---|---|---|---|---|---|---|
| Anchor type | | Mechanical anchorage | | | | | | |
| Concrete strength (MPa) | | 49.4 | 51.6 | 51.1 | 64.3 | 60.8 | 62.6 | 62.6 |
| Column (250×250mm) | Longitudinal steel bars | 12-D25(SD345) | | | 12-D22(SD345) | | | |
| | Tie | 4-D10@100 (SD785) | 4-D10@100 (SD390) | 2-D10@100 (SD295A) | 4-D10@100(SD390) | | | |
| | Height(mm) | 2700 | | | | | | |
| Beam (225×275mm) | Longitudinal steel bars | 5-D25@100(SD490) | | | | | | |
| | Stirrup | 3-D10@100(SD295A) | | | | | | |
| | Span(mm) | 3700 | | | | | | |
| Joint transverse reinforcement bars | | 4-D10 4set (SD785) | 4-D10 4set (SD390) | 2-D10 4set (SD295A) | 4-D10 4set (SD785) | 4-D13 4set (SD390) | 4-D13 4set (SD295A) | 4-D10 4set (SD390) |
| Joint transverse reinforcement ratio | | 0.72 | 0.38 | 0.15 | 0.70 | 0.61 | 0.51 | 0.40 |
| Shear reinforcement ratio $\rho_w$ (%) | Column | 0.57 | | 0.25 | 0.57 | | | |
| | Beam | 0.48 | | | | | | |
| | Joint | 0.50 | | 0.29 | 0.50 | 0.88 | | 0.50 |
| Column-to-beam moment capacity ratio | + | 1.76 | 1.77 | 1.77 | 1.52 | 1.51 | | |
| | - | 1.52 | | | 1.23 | | | |
| $\beta_j$ | + | 1.22 | 1.06 | 0.94 | 1.16 | 1.11 | 1.07 | 1.02 |
| | - | 1.16 | 1.00 | 0.89 | 1.11 | 1.06 | 1.01 | 0.96 |

Table 2 List of specimens with varying axial force (1)

| Test specimen | | T15-60 T6C5 | T15-60 T6C5 | T12-60 T6C5 | T12-40 T6C5 | T12-20 T6C5 | T12-20 T6C3 | T12-15 T6C5 | T12-15 T6C3 |
|---|---|---|---|---|---|---|---|---|---|
| Anchor type | | Mechanical anchorage | | | | | | | |
| Concrete strength (MPa) | | 64.9 | 65.0 | 64.9 | 75.2 | 64.9 | 60.9 | 76.0 | 75.0 |
| Column (250×250 mm) | Longitudinal steel bars | 12-D16 (SD490) | | | 12-D16 (SD345) | | | | |
| | Tie | 2-D6@50(SD295A) | | | | | | | |
| | Height(mm) | 1350 | | | | | | | |
| Beam (225×275 mm) | Longitudinal steel bars | 5-D13(SD490) | | | | | | | |
| | Stirrup | 3-D6@50(SD295A) | | | | | | | |
| | Span(mm) | 1850 | | | | | | | |
| Joint transverse reinforcement bars | | 4-D6 4set (SD345) | 2-D6 3set (SD295A) | 4-D6 4set (SD345) | 2-D6 5set (SD295A) | 2-D6 3set (SD295A) | | 2-D6 2set (SD295A) | |
| Joint transverse reinforcement ratio | | 0.59 | 0.23 | 0.59 | 0.41 | 0.24 | 0.23 | 0.16 | |
| Shear reinforcement ratio $\rho_w$ (%) | Column | 0.51 | | | | | | | |
| | Beam | 0.84 | | | | | | | |
| | Joint | 0.92 | 0.34 | 0.92 | 0.57 | 0.34 | | 0.23 | |
| Varying axial force ratio | $\rho_C$ | 0.47 | 0.28 | 0.47 | 0.45 | 0.47 | 0.28 | 0.44 | 0.30 |
| | $\rho_T$ | -0.62 | -0.62 | -0.64 | -0.61 | -0.64 | -0.64 | -0.61 | -0.61 |
| Column-to-beam moment capacity ratio | + | 4.51 | | 4.29 | 4.59 | 4.16 | 4.29 | 4.64 | 4.72 |
| | - | 1.54 | | 1.27 | 1.22 | 1.27 | 1.27 | 1.22 | |
| $\beta_j$ | + | 1.69 | 1.52 | 1.67 | 1.66 | 1.48 | 1.49 | 1.55 | 1.56 |
| | - | 1.12 | 0.94 | 1.06 | 0.97 | 0.87 | 0.88 | 0.85 | 0.85 |

beam-column joint, while the following *T* and *C* are the abbreviations of tension and compression. As shown in the Fig. 2, the side loaded with compressive axial force for the joint is defined as positive side (+). The other is considered as negative side (-). The subsequent numbers 15 and 30 mean the column-to-beam moment capacity ratio and the joint transverse reinforcement ratio respectively. Finally, the 6 and 4 are values of compressive axial force ratio and tensile axial force ratio respectively.

The names of specimens with non-axial force consist of

Table 3 List of specimens with varying axial force (2)

| Test specimen | | T15-30T6C4 | T15-15T6C2 | T12-30T6C4 | T12-30T6C3 | T12-20T6C2 | T12-15T6C2 |
|---|---|---|---|---|---|---|---|
| Anchor type | | Mechanical anchorage | | | | | |
| Concrete strength (MPa) | | 93.3 | 94.8 | 94.9 | 95.1 | | 94.8 |
| Column (250×250 mm) | Longitudinal steel bars | 12-D16(SD490) | | 12-D16(SD345) | | | |
| | Tie | 2-D6@50(SD295A) | | | | | |
| | Height(mm) | 1350 | | | | | |
| Beam (225×275 mm) | Longitudinal steel bars | 5-D13(SD490) | | | | | |
| | Stirrup | 3-D6@50(SD295A) | | | | | |
| | Span(mm) | 1850 | | | | | |
| Joint transverse reinforcement bars | | 2-D6 4set (SD295A) | 2-D6 2set (SD295A) | 2-D6 4set (SD295A) | | 2-D6 3set (SD295A) | 2-D6 2set (SD295A) |
| Joint transverse reinforcement ratio | | 0.31 | 0.15 | 0.31 | | 0.23 | 0.15 |
| Shear reinforcement ratio $\rho_w$ (%) | Column | 0.51 | | | | | |
| | Beam | 0.84 | | | | | |
| | Joint | 0.46 | 0.23 | 0.46 | | 0.34 | 0.23 |
| Varying axial force ratio | $\rho_C$ | 0.36 | 0.18 | 0.36 | 0.27 | 0.18 | |
| | $\rho_T$ | -0.61 | | | | | |
| Column-to-beam moment capacity ratio | + | 5.59 | 5.22 | 5.53 | | 5.34 | 4.82 |
| | - | 1.57 | 1.57 | 1.24 | | 1.24 | 1.24 |
| $\beta_j$ | + | 1.82 | 1.67 | 1.81 | | 1.77 | 1.62 |
| | - | 1.01 | 0.93 | 0.94 | | 0.94 | 0.90 |

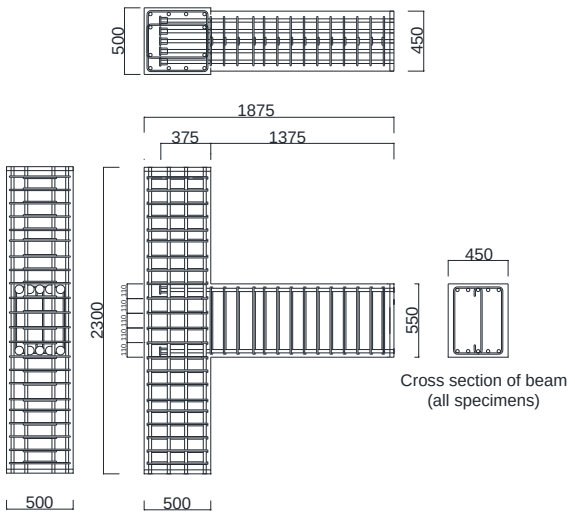


Fig. 3 Reinforcement detail of specimens with non-axial force

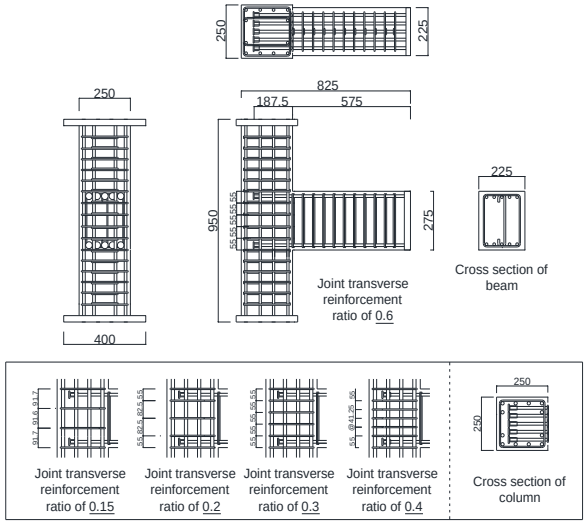


Fig. 4 Reinforcement detail of specimens varying axial force

the value of column-to-beam moment capacity ratio and joint transverse reinforcement ratio. The positive and negative sides of specimens with non-axial force are the same directions of horizontal loading as that of specimens with varying axial force.

The parameters of each specimen are shown in the Table.1-3. The reinforcement detail drawings are shown in Figs. 3-4. The mechanical anchorage is applied to all specimens. Based on the AIJ Standard for Structural Calculation of Reinforced Concrete Structures (2010), the development length is set to be 3/4 of depth of column.

Referring to the AIJ Standard for Lateral Load-carrying Capacity Calculation (2016) and the previous research (Shiohara 2004), the judging criteria of beam-column joint failure is defined as follows:

1) The maximum experimental value of story shear force is smaller than its theoretical value; 2) large deformation of joint panel is observed; 3) yielding of beam longitudinal steel bars, transverse reinforcement bars and column longitudinal steel bars within joint area are observed.

Referring to the Guidelines for Performance Evaluation

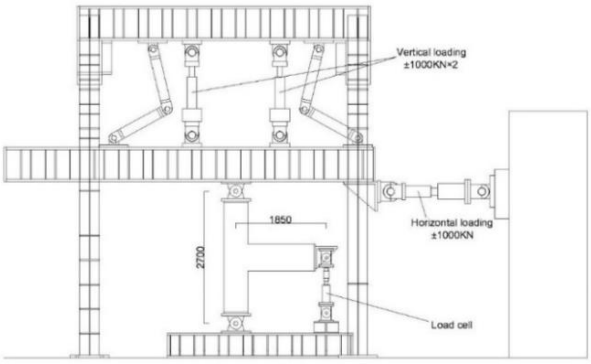


Fig. 5 Loading test machine for specimens with non-axial force

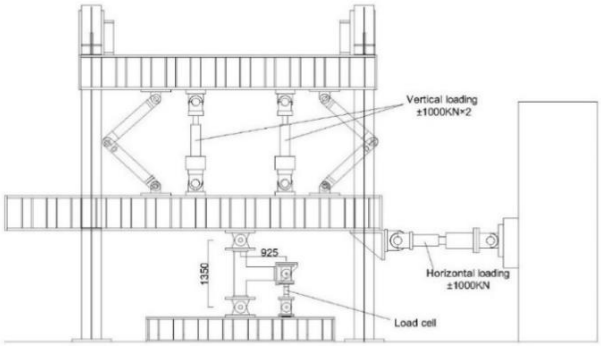


Fig. 6 Loading test machine for specimens with varying axial force

of Earthquake Resistant Reinforced Concrete Buildings (2004) and previous studies (Kabeyasawa 2002, Yoshimura 2004), the judging criteria of axial collapse is defined as follows:

1) The increase of shear crack width and extensive spalling have been observed with a loss of axial load carrying capacity; 2) The story shear force deterioration down to 80% or less from the maximum value.

### *2.2 Experimental setup*

The loading equipment of specimens with non-axial force and axial force are installed as shown in Fig. 5 and Fig. 6. In each test, the top and the bottom of columns are supported by pin joints while the end of the beam is supported by a horizontal roller. The three points in this frame are the inflection points of the columns and beam. Regarding the loading method, specimens are subjected to static cyclic loading through horizontal and vertical hydraulic jacks linked to the steel frame beam at top of column. In these figures, the side in which the horizontal jack pushed forward to the left side resulting in compressive loading for the joint is defined as positive side (+). The other loading direction is considered as negative side (-). Horizontal loading is carried out according to the cycle shown in Fig. 7. As shown in Fig. 8, varying axial force ($N$) is applied proportionally to beam shear force ($Q_b$). But for specimens with non-axial force, except axial force produced by the rotation of the specimen during the loading, no extra axial force is loaded.

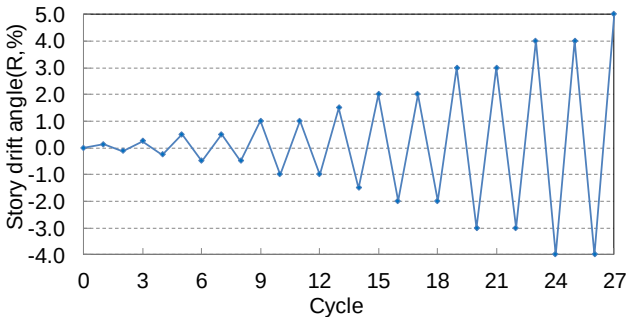


Fig. 7 Horizontal loading cycle

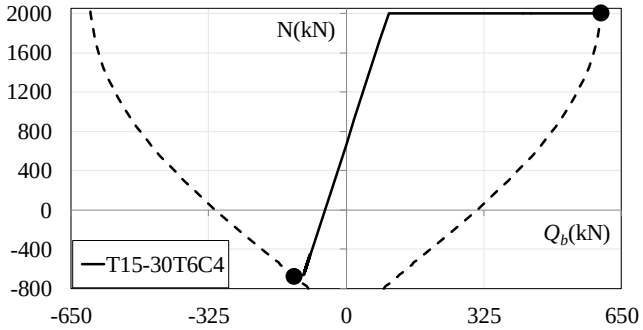


Fig. 8 Axial force loading method

## 3. Experimental result

### *3.1 Story shear force-story drift angle*

In Figs. 9-11, the relations between story shear force and story drift angle of each specimen are shown. The story shear force is obtained through moment equilibrium between the measured beam shear force and the horizontal force at the loading point on the top of column. The story drift angle is calculated as lateral displacement at top of the column divided by the height of specimen.

Critical points are marked with corresponding symbols. The hysteresis characteristics of all specimens show a comparatively spindle-shaped loops when the story drift angle is less than 0.5%. But it gradually changes into S-shape (Nogami 2012) with the development of loading. The other details of each specimen are described as follows:

For specimens with non-axial force, the hysteresis loops show similar characteristics on both sides of loading. When the joint transverse reinforcement ratio and the column-to-beam moment capacity ratio are set to be a lower level, there is a tendency that the transverse reinforcement bars in joint and longitudinal steel bars in the column yield earlier than that of longitudinal steel bars at beam. The reduction of story shear force is also observed for all specimens except the specimen T15-70 after the story drift angle of maximum experimental values of story shear force. For specimen T15-70, the yield point of longitudinal steel bars in the beam happens earlier than transverse reinforcement bars in the joint on the both sides of loading. Meanwhile, the maximum experimental values of story shear force on the both sides of loading are larger than its theoretical values which reveals an evidence of beam yield mechanism.

For specimens with varying axial force, the hysteresis

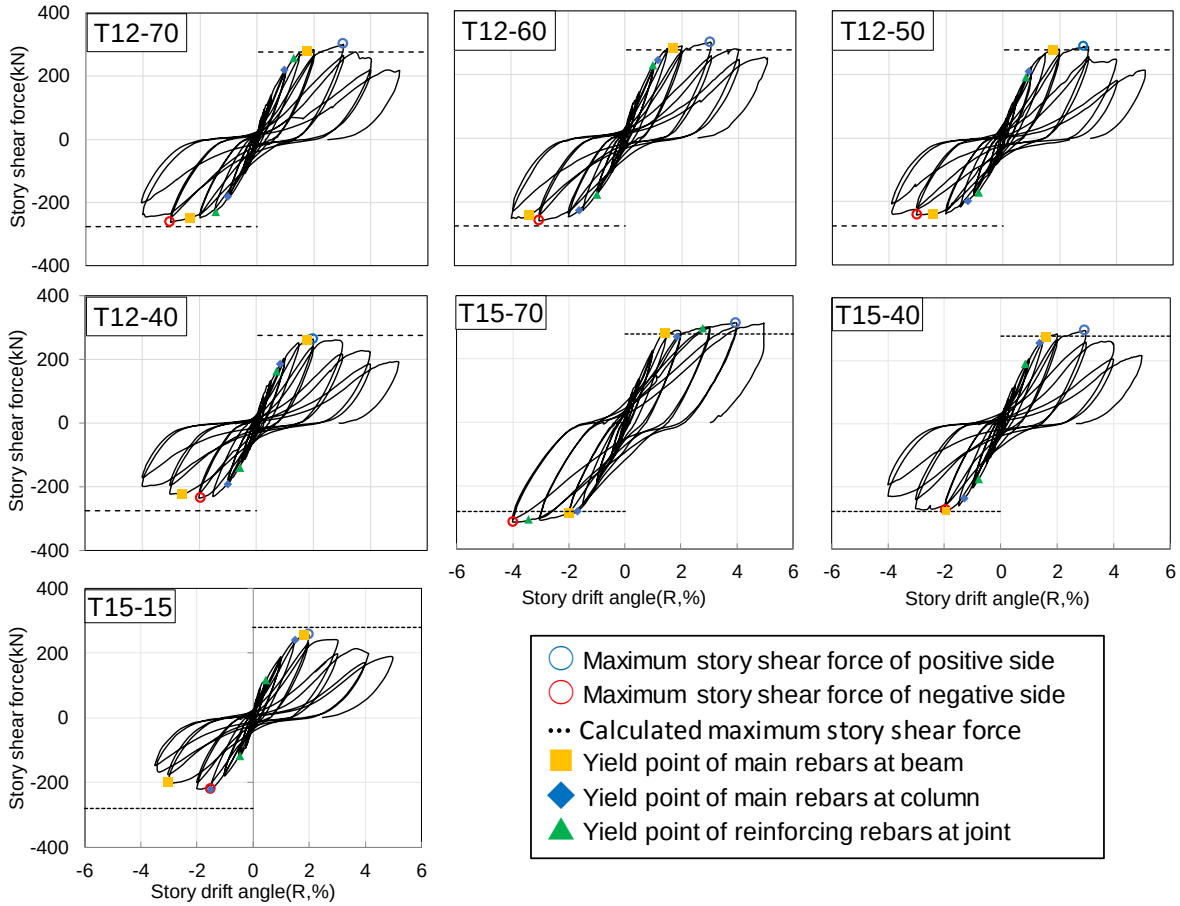


Fig. 9 Story shear force-story drift angle relation of specimens with non-axial force

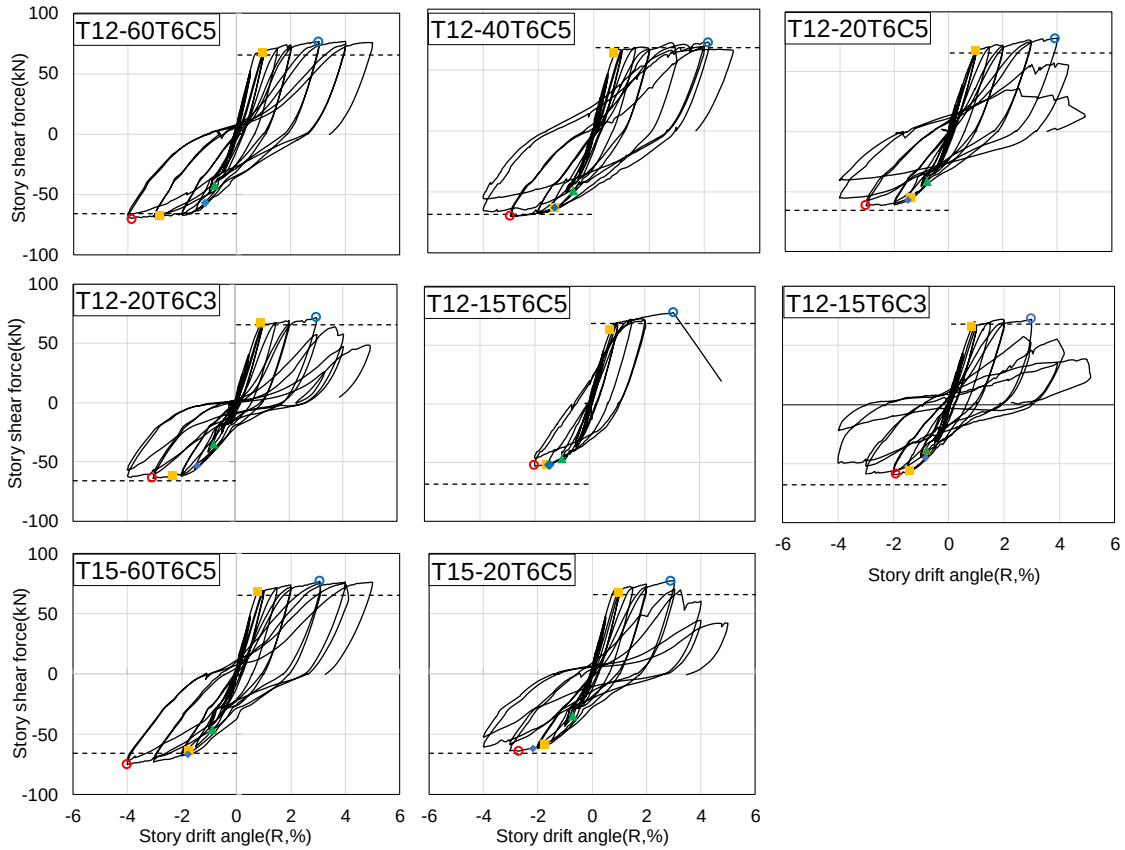


Fig. 10 Story shear force-story drift angle relation of specimens with varying axial force (1)

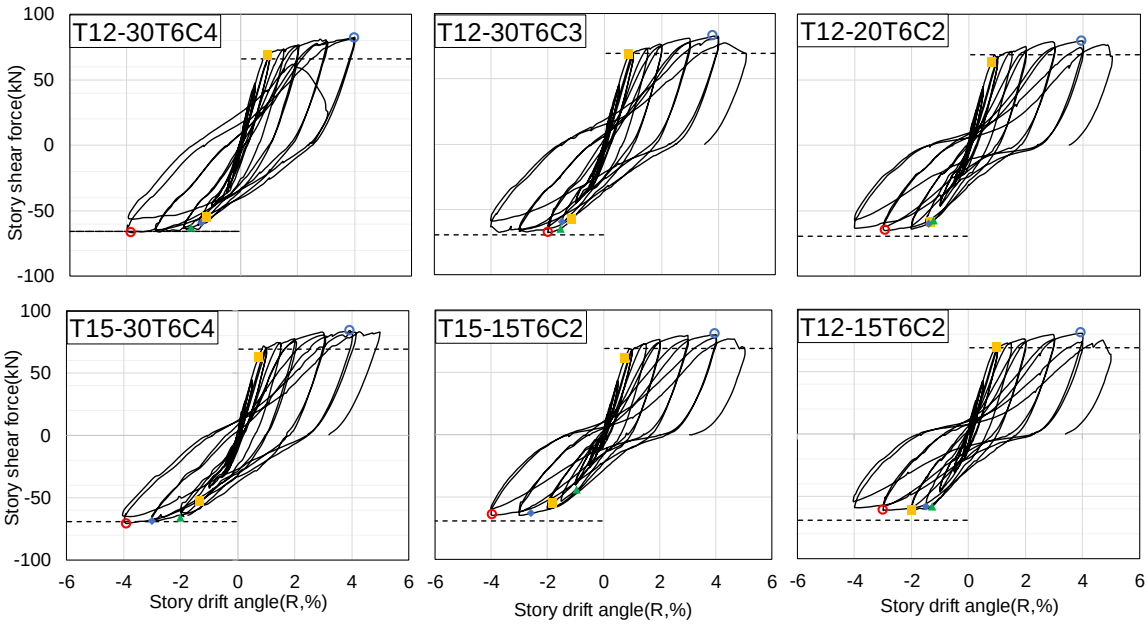


Fig. 11 Story shear force-story drift angle relation of specimens with varying axial force (2)

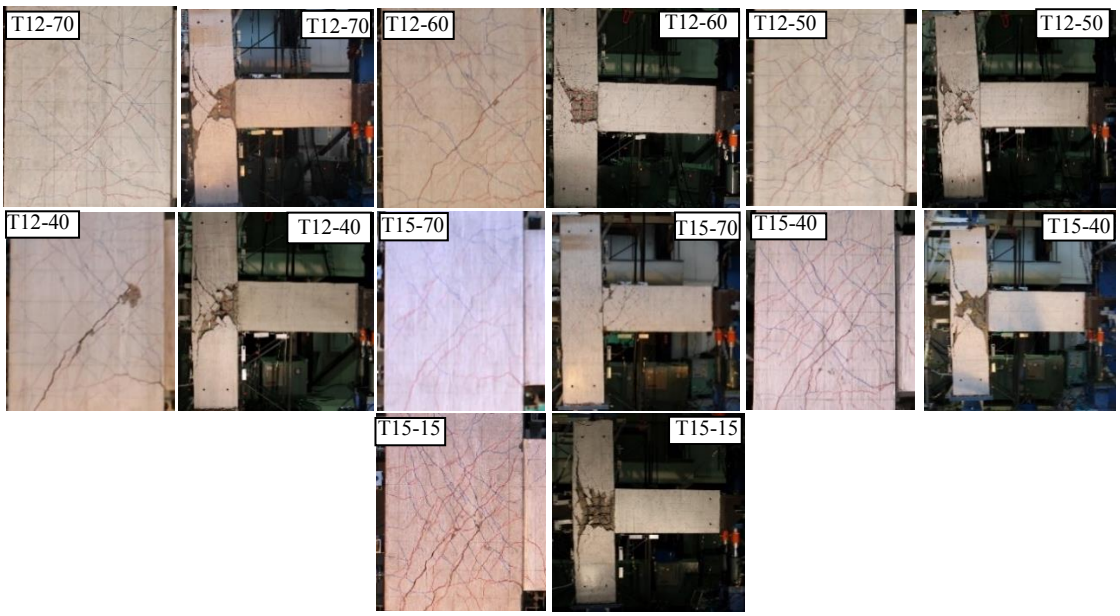


Fig. 12 Damage and cracking mode of specimens with non-axial force
(Left: story drift angle of -2.0%, Right: ultimate deformation)

loops on the positive side and the negative side show different results. On the positive side, the longitudinal reinforcement bars in the top beam of all specimens yield at a story drift angle of 1.0%. The maximum experimental values of story shear force are larger than its theoretical values for all specimens at a story drift angle of 3.0% or 4.0%. After that, the loss of lateral load-carrying capacity is observed for specimens with varying axial force except specimens T15-60T6C5, T15-60T6C5, T12-60T6C5 and T12-40T6C5. Moreover, for specimens T15-20T6C5, T12-30T6C4, T12-20T6C5, T12-20T6C3, T12-15T6C5 and T12-15T6C3, no additional axial force can be resisted by the frame during the final cycle of ultimate deformation as an axial collapse occurred.

On the negative side, the maximum experimental values of story shear force are obviously affected by the joint transverse reinforcement ratio. For specimens with lower joint transverse reinforcement ratios (0.15-0.2), the maximum experimental values of story shear force are smaller than its theoretical values. The transverse reinforcement bars at joint yield at a story drift angle of 1.0% or 1.5% earlier than that of longitudinal steel bars in the bottom beam, which shows a tendency of joint failure. On the other hand, for specimens T15-60T6C5, T15-60T6C5, T12-60T6C5 and T12-40T6C5, maximum experimental values of story shear force are larger than theoretical values. Moreover, for these 4 specimens, no evident loss of lateral load-carrying capacity is observed

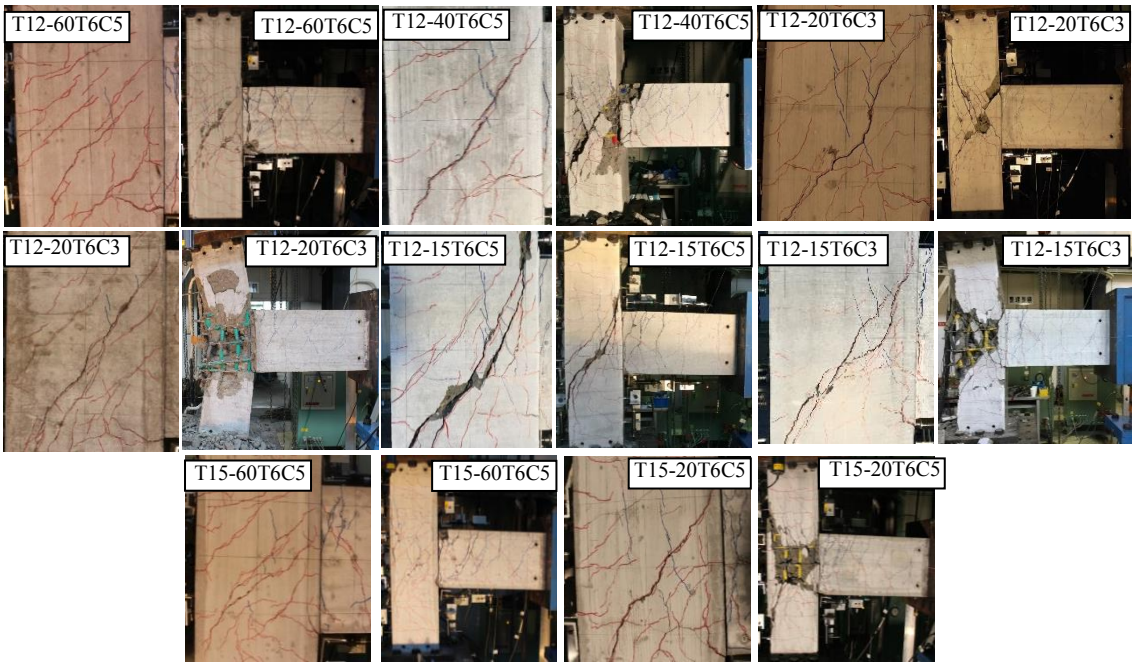


Fig. 13 Damage and cracking mode of specimens with varying axial force (1)
(Left: story drift angle of -2.0%, Right: ultimate deformation)

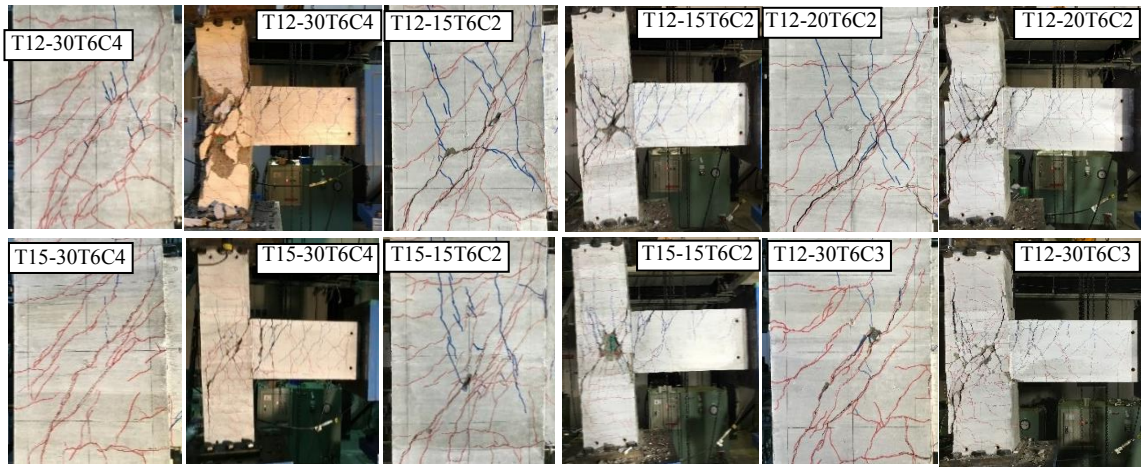


Fig. 14 Damage and cracking mode of specimens with varying axial force (2)
(Left: story drift angle of -2.0%, Right: ultimate deformation)

after the story drift angle of maximum story shear force.

### *3.2 Damage situation*

In Fig. 12-14, the damage situation of each specimen at a story drift angle of -2.0% and ultimate deformation are shown. The cracks produced on positive side are recorded by blue marks, the negative side in red marks.

For specimens with non-axial force, the crossed-diagonal cracks produced on the both sides in the joint panel are observed. The width of cracks on both sides are restrained with the increase of joint transverse reinforcement ratio. Even with the same joint transverse reinforcement ratio, the damage is obviously affected by the increase of column-to-beam moment capacity ratio. Unlike the extensive spalling in the joint panel of specimen T12-70, the damage is observed to concentrate at the beam for specimen T15-70.

For specimens with varying axial force, the effect of increasing the joint transverse reinforcement ratio is also verified. Unlike the cross-diagonal cracks produced in the joint panel of specimens with non-axial force, cracks of specimens with varying axial force produced on positive loading are found to be perpendicular to the horizontal line of joint panel. The width of cracks on the positive side are apparently restrained compared with those on the negative side.

For specimens with higher compressive axial force ratio, the width of cracks is narrower than that of specimens with lower compressive axial force ratio. It can be concluded that even though axial collapse may happen during the final cycle of ultimate deformation. When story drift angle is less than 2.0%, the deformation of the joint panel on the positive loading can be effectively restrained.

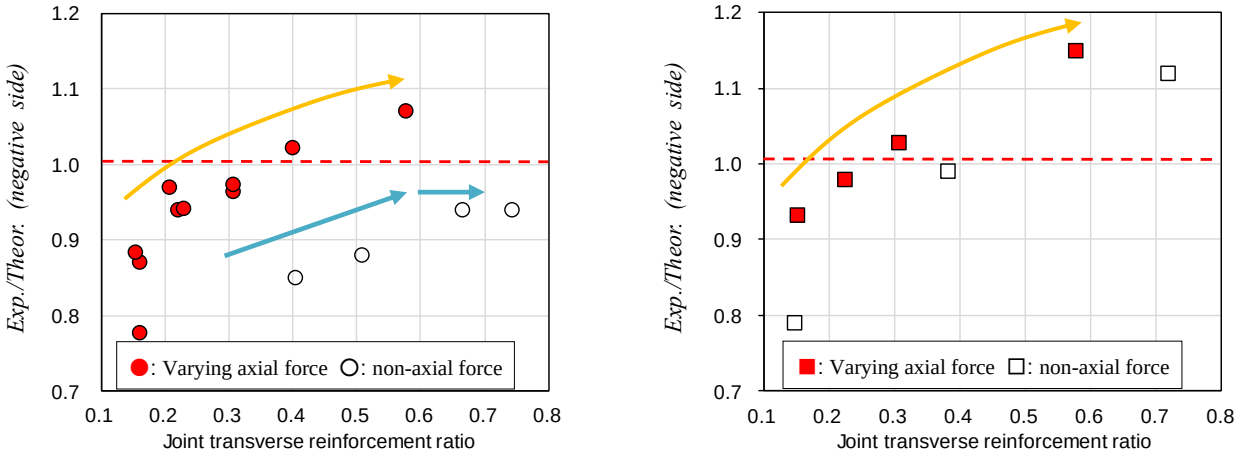


(a) Column-to-beam moment capacity ratio≒1.2 (b) Column-to-beam moment capacity ratio≒1.5

Fig. 15 Ratio of experimental value to theoretical value - joint transverse reinforcement ratio

Moreover, when joint transverse reinforcement ratio is set in the range of 0.15 to 0.2, severe shear cracks and extensive spalling in the joint panel occur which increases the risk of axial collapse during the final cycle of ultimate deformation.

## 4. Influence of each parameter

### *4.1 Lateral load-carrying capacity*

#### *4.1.1 Story shear force*

In the previous analysis, it has been demonstrated that the maximum experimental values of story shear force on the negative side of most specimens are smaller than its theoretical values which probably results in the joint failure and the axial collapse. With the increase of joint transverse reinforcement ratio, the risk can be effectively reduced. To define this boundary of required joint transverse reinforcement ratio, the relation between the ratio of maximum experimental values of story shear force to its theoretical values on the negative side and joint transverse reinforcement ratio is analyzed by all specimens with non-axial force and varying axial force.

In Fig. 15, it can be concluded that the ratio of maximum experimental values of story shear force to its theoretical values increased as joint transverse reinforcement ratio increased. However, there are differences in the effect of reinforcement between specimens with non-axial force and varying axial force.

For the specimens with non-axial force when column-to-beam moment capacity ratio is 1.2, the maximum experimental values of story shear force are smaller than theoretical values. The ratio of maximum experimental values of story shear force to theoretical value remains constant around 0.94 when the joint transverse reinforcement ratio is more than 0.61.

For specimens with varying axial force, the ratio of maximum experimental value of story shear force to its theoretical value is equal to 1.02 when the joint transverse reinforcement ratio is 0.41. The ratio of maximum experimental value of story shear force to theoretical value increases by 4.9% as the joint transverse reinforcement ratio increased from 0.41 to 0.59.

For specimens with the column-to-beam moment capacity ratio of 1.5, the ratio of maximum experimental values of story shear force to its theoretical value increases for both varying axial force specimens and non-axial force specimens compared with specimens with the column-to-beam moment capacity ratio of 1.2. For non-axial force specimens, the ratio of maximum experimental value of story shear force to its theoretical value is approximately equal to 1.0 when the joint transverse reinforcement ratio is 0.38.

For specimens with varying axial force, the ratio of maximum experimental value of story shear force to its theoretical value is equal to 1.03 when the joint transverse reinforcement ratio is 0.31. The ratio of maximum experimental value of story shear force to its theoretical value increases by 11.7% as the joint transverse reinforcement ratio increased from 0.31 to 0.59.

#### *4.1.2 Evaluation of $\beta_j$*

According to the AIJ Standard for Lateral Load-carrying Capacity Calculation (2016), the ratio of maximum experimental value of story shear force to its theoretical value of beam-column joint can be predicted by a factor $\beta_j$. The factor $\beta_j$ for the exterior beam-column joint is shown as follows

$$\beta_j = \left\{ 0.85 - \frac{\sum A_t f_y}{b_j D_b F_c} + \frac{1}{4}\left( \frac{M_{cu1} + M_{cu2}}{M_{bu}} \xi_a - 1 \right) + \frac{1}{2}\left( \frac{\sum A_{jw} f_{jy}}{\sum A_t f_y} \right) \right\} \xi_r \qquad (5)$$

where $\Sigma A_t$ is the total section area of the joint transverse reinforcement bars, $f_y$ is the yield point of transverse reinforcement bars, $b_j$ is the effective width of beam-column joint section, $D_b$ is depth of beam section, $F_c$ is the strength of concrete, $M_{cu1,2}$ are ultimate nodal bending moments of the upper and lower columns respectively, $M_{bu}$ is ultimate nodal bending moments of the beam, $\xi_a$ is the effective depth ratio of column section ($=D_{jc}/D_c$), $\Sigma A_{jw}$ is the total section area of beam longitudinal reinforcement bars

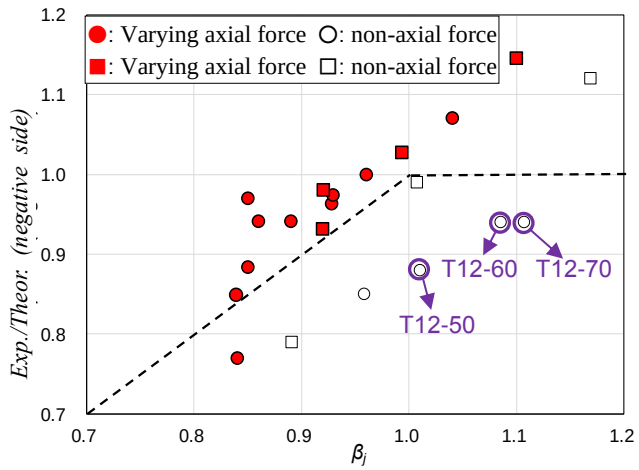


Fig. 16 Ratio of experimental value to theoretical value-$\beta_j$ (●,○: Column-to-beam moment capacity ratio≒1.2, ■,□: Column-to-beam moment capacity ratio≒1.5)

on the tension side, $f_{jy}$ is the yield point of beam longitudinal steel bars, $\xi_r$ is the correction factor according to the aspect ratio of beam-column joint, $D_{jc}$ is the effective length of beam-column joint section in the horizontal direction, $D_c$ is depth of column section.

The longitudinal steel bars of the tensile side, strength of concrete, column-to-beam moment capacity ratio, joint transverse reinforcement ratio and dimensions of joint are considered as the parameters which affect the ratio of maximum experimental story shear force to theoretical value. However, the axial force which proved to improve the lateral load-carrying capacity of joint frame is not considered in the formula. Therefore, it is necessary to verify the validity of $\beta_j$ through the results of specimens with non-axial force and varying axial force.

In Fig. 16, the relation between the ratio of maximum experimental values of story shear force to its theoretical value and $\beta_j$ on the negative side is shown. For non-axial force specimens, the ratios of maximum experimental values of story shear force to the theoretical value are underestimated by $\beta_j$. When the column-to-beam moment capacity ratio is 1.2 and the transverse reinforcement ratio is increased to be over 0.51, the failure modes of specimens are mistakenly evaluated, which is considered unsafe in design.

For most varying axial force specimens, although the values of $\beta_j$ are slightly smaller than the ratios of maximum experimental values of story shear force to the theoretical values, the failure modes of specimens are well predicted.

### 4.2 Axial load-carrying capacity

In this section, all the specimens with varying axial force are selected and the boundaries of beam-column joint failure and axial collapse when given the column-to-beam moment capacity ratios of 1.2 and 1.5 are studied. The combination effect of column-to-beam moment capacity ratio, joint transverse reinforcement ratio and compressive axial force ratio are discussed.

Fig. 17 shows the relation between compressive axial force and joint transverse reinforcement ratio for specimens with varying axial force when column-to-beam moment capacity ratios are 1.2 and 1.5 respectively. The shaded areas represent the predicted the areas of axial collapse it is concluded that for specimens with low joint transverse reinforcement ratios (0.15-0.2) and the least compressive axial force ratio (0.18), the axial compressive force can be maintained until the story drift angle of +5.0% without axial collapse. When the transverse reinforcement ratio is less than 0.31, the mode of failure is proved to be the joint failure. In addition, when the compressive axial force ratio is increased above 0.36, the axial collapse is observed. Moreover, neither beam-column joint failure nor axial collapse are observed for specimens with transverse reinforcement ratios greater than 0.41.

On the other hand, there are only 4 specimens with column-to-beam moment capacity ratio of 1.5 loaded with varying axial force. Therefore, more specimens should be conducted to draw the definite conclusions. When transverse reinforcement ratio is set to be over 0.31, it is inferred that the beam-column joint failure and the axial collapse can be prevented under the highest compressive axial force ratio. Comparing the experimental results of specimens T15-30T6C4 and T12-30T6C4, the increase of column-to-beam moment capacity ratio can also effectively avoid the beam-column joint failure and axial collapse.

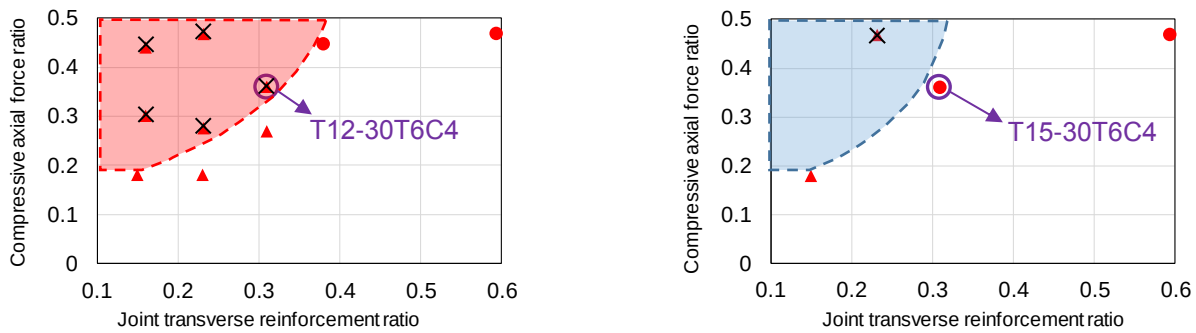


(a) Column-to-beam moment capacity ratio≒1.2 (b) Column-to-beam moment capacity ratio≒1.5

Fig. 17 Compressive axial force ratio - joint transverse reinforcement ratio

(● : Non-beam-column joint flexural failure, ▲ : Beam-column joint flexural failure, × : Axial collapse)

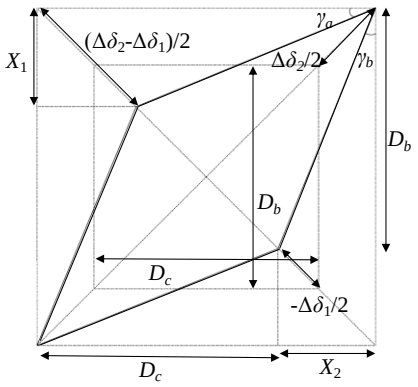


Fig. 18 Shear deformation diagram of joint panel

### *4.3 Deformation*

#### *4.3.1 Shear deformation of joint panel*

In this section, the reinforcing effect is evaluated by comparing the shear deformation of joint panels among specimens with varying high axial force. As illustrated in Fig. 18, the shear deformation angle $\gamma$ on the negative side is calculated according to the diagonal concrete strut action mechanism (Paulay 1978, Macgregor 1988, Arthur *et al.* 2003).

$$\gamma_a = \frac{X_1}{D_c} = \frac{D_b \cdot (\Delta\delta_2 - \Delta\delta_1)}{2D_c\sqrt{D_b^2 + D_c^2}} \tag{6}$$

$$\gamma_b = \frac{X_2}{D_b} = \frac{D_c \cdot (\Delta\delta_2 - \Delta\delta_1)}{2D_b\sqrt{D_b^2 + D_c^2}} \tag{7}$$

$$\gamma = \gamma_a + \gamma_b = \frac{\sqrt{D_b^2 + D_c^2}\,(\Delta\delta_2 - \Delta\delta_1)}{2D_b \cdot D_c} \tag{8}$$

Where $D_b$, $D_c$ are the effective width and length of joint panel, $\Delta\delta_1$, $\Delta\delta_2$ are the length change of diagonal line at joint panel.

In Fig. 19, specimens with large varying axial force (-0.6~0.36-0.47) are compared at main story drift angles on the negative side. A decrease relation between the shear deformation angle of joint panel and the joint transverse reinforcement ratio is observed.

For specimens with a column-to-beam moment capacity ratio of 1.2, regardless of what the joint transverse reinforcement ratio is, there is no obvious difference in the shear deformation for story drift angle of -0.5% and -1.0%. For the specimens with transverse reinforcement ratios less than 0.31, drastic shear deformations are observed. Moreover, for the specimens with a joint transverse reinforcement ratio of 0.16, the deformation of the joint

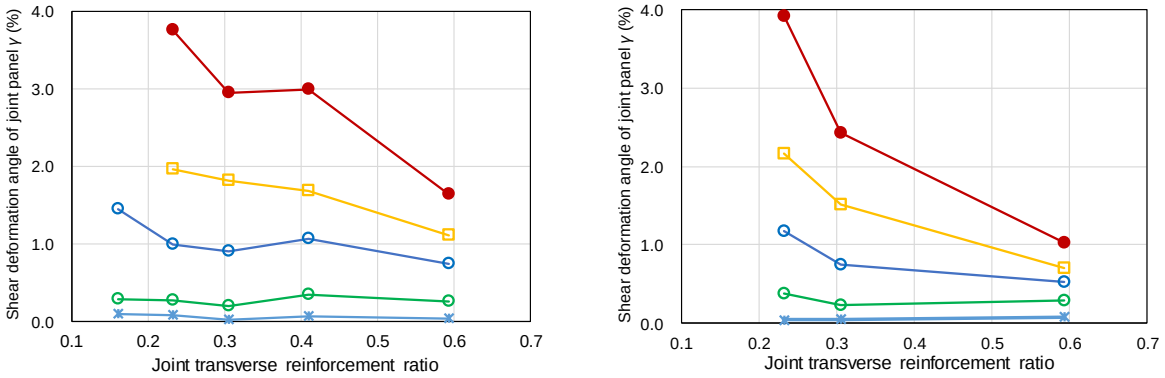


(a) Column-to-beam moment capacity ratio≒1.2 (b) Column-to-beam moment capacity ratio≒1.5

Fig. 19 Shear deformation angle of joint panel -joint transverse reinforcement ratio
( -0.5% -1.0% -2.0% -3.0% -4.0% )

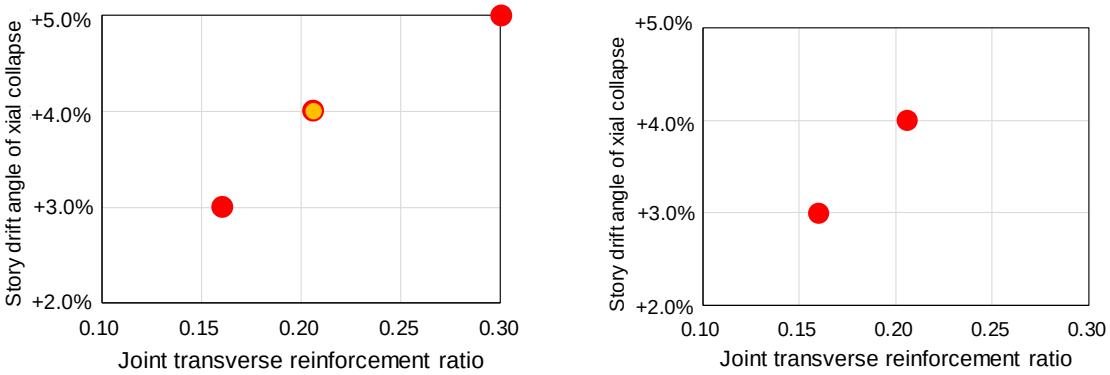


(a) Varying axial force ratio:(-0.6~0.4, 0.5) (b) Varying axial force ratio:(-0.6~0.3)

Fig. 20 Story drift angle of axial collapse - joint transverse reinforcement ratio
(●:Column-to-beam moment capacity ratio≒1.2 ●:Column-to-beam moment capacity ratio≒1.5)

panel increases by 64.2% from the story drift angles of -0.5% to -1.0%. An axial collapse occurs after the story drift angles of -2.0%. Even though the shear deformation angles are almost the same at a story drift angle of -4.0% for specimens with transverse reinforcement ratio of 0.31 and 0.41, the beam-column joint failure and axial collapse can be prevented by increasing the joint transverse reinforcement ratio.

When the column-to-beam moment capacity ratio is 1.5, a similar tendency is observed as that of 1.2. But with the increase of column-to-beam moment capacity ratio, the shear deformation is evidently restrained. For instance, if the transverse reinforcement ratio is increased to 0.31, the shear deformation angle at a story drift angle of -4.0% is reduced by 19.0% compared with that of the column-to-beam moment capacity ratio of 1.2.

#### *4.3.2 Story drift angle at axial collapse*

As illustrated in Fig. 20, the relation between the story drift angle of axial collapse occurred and joint transverse reinforcement ratio is shown.

It is concluded that the axial collapse is not observed for story drift angles less than 2.0% even with the lowest joint transverse reinforcement ratio and regardless of the compressive axial force ratio. Meanwhile, as the joint transverse reinforcement ratio increases, the axial collapse tends to occur at a larger story drift angle.

## 5. Conclusions

The objective of this study is to investigate the effect of varying axial force on the seismic performance of beam-column joint. Through the testing of 7 full-scale specimens with non-axial force and 14 half-scale specimens with varying axial force subjected to static loading tests, the following conclusions can be made:

- Compared to the specimens with non-axial force, specimens with varying axial force are proved to have better performance on lateral load-carrying capacity. When column-to-beam moment capacity ratios are 1.2, for specimens with non-axial force, the maximum experimental values of story shear force could not reach its theoretical values, even if the joint transverse reinforcement ratio is increased to 0.70. For varying axial force specimens, if the joint transverse reinforcement ratio is over 0.41, the maximum experimental value of story shear force is larger than its theoretical value. Meanwhile, the loss of lateral load-carrying capacity and the joint failure can be effectively avoided. When column-to-beam moment capacity ratio is 1.5, for specimens with non-axial force, the maximum experimental value of story shear force is slightly less than its theoretical value if the joint transverse reinforcement ratio is increased to 0.38. For varying axial force specimens, the loss of lateral load-carrying capacity and the joint failure can be avoided, if the joint transverse reinforcement ratio is over 0.31.
- For specimens with varying axial force, the failure modes are well predicted by using $\beta_j$. But for specimens with non-axial force, the ratios of maximum experimental story shear force to theoretical value are underestimated.
- When the compressive axial force ratio is less than 0.18, for specimens with a column-to-beam moment capacity ratio of 1.2 and a joint transverse reinforcement ratio of 0.15, the axial collapse is not observed. When the compressive axial force ratio is approximately 0.47, the joint transverse reinforcement ratio is needed to be above 0.41 to prevent the axial collapse. For specimens with a column-to-beam moment capacity ratio of 1.5, to prevent the axial collapse, the lower limit of joint transverse reinforcement ratio is predicted to be at a range of 0.31-0.41.
- Under varying high axial force, the increase of joint transverse reinforcement ratio contributes significantly to restraining the shear deformation of joint panel and delaying axial collapse.

## Acknowledgments

The research was financially and technically supported by Horie Engineering and Architectural Research Institute Co., Ltd., Tokyo Tekko Co., Ltd., Asahi Industries Co., Ltd., and Suzuki Architectural Design Office. Discussions with the researchers from Yokohama National University, Osaka University, Shibaura Institute of Technology, Huazhong University of Science and Technology, Purdue University, and Wuhan University of Technology are gratefully acknowledged.

## References

ACI 318 (2011), Building Code Requirements for Structural Concrete and Commentary, American Concrete Institute, Farmington Hills, MI, USA.

AIJ Standard for Lateral Load-carrying Capacity Calculation of Reinforced Concrete Structures (2016), Architectural Institute of Japan, Tokyo, Japan.

AIJ Standard for Structural Calculation of Reinforced Concrete Structures (2010), Architectural Institute of Japan, Tokyo, Japan.

Arthur, N., David, D. and Charles, D. (2003), *Design of Concrete Structure*, 13th Edition, McGraw-Hill, New York, NY, USA.

Elwood, K.J. and Moehle, J.P. (2005), "An axial capacity model for shear-damaged columns", *ACI Struct. J.*, **102**(4), 145-166. https://doi.org/10.14359/14562.

Eurocode (2003), Design Provisions for Earthquake Resistant Structures. Part 1: General Rules, Seismic Actions and Rules for Buildings, European Committee for Standardization, Brussels, Belgium.

Fu, J.P., Chen, T., Wang, Z. and Bai, S.L. (2000), "Effect of axial load ratio on seismic behaviour of interior beam-column joints", *Proceedings of 12th WCEE*, Auckland, New Zealand, February.

Fujii, S. and Morita, S. (1991), "Comparison between interior and exterior R/C beam-column joint behavior", *ACI Spec. Publ.*, **123**(6), 145-166. https://doi.org/10.14359/2836.

Guidelines for Performance Evaluation of Earthquake Resistant Reinforced Concrete Buildings (2004), Architectural Institute of Japan, Tokyo, Japan.

Henkhaus, K., Pujol, S. and Ramirez, J. (2013), "Axial failure of reinforced concrete 23 columns damaged by shear reversals", *J.*

*Struct. Eng.*, **139**(7), 1172-1180. https://doi.org/10.1061/(ASCE)ST.1943-541X.0000673.

Hwang, S.J., Lee, H.J. and Wang, K.C. (2004), "Seismic design and detailing of exterior reinforced concrete beam-column joints", *Proceedings of 13th WCEE*, Vancouver, B.C., Canada, August.

Kabeyasawa, T., Tasai, A. and Igarashi, S. (2002), "An economical and efficient method of strengthening reinforced concrete columns against axial load collapse during major earthquake", *Third US-Japan Workshop on Performance-Based Earthquake Engineering Methodology for Reinforced Concrete Building Structures*, Seattle, USA, February.

Kim, C.G., Park, H.G., Eom, T.S. and Kim, T.W., (2015), "Effect of shear reinforcement on seismic performance of RC beam column joints", *Proceedings of the Tenth Pacific Conference on Earthquake Engineering Building an Earthquake-Resilient Pacific*, Sydney, Australia, November.

Kusuhara, F. and Shiohara, H. (2010), "Ultimate moment of reinforced concrete interior beam-column joint", *J. Struct. Constr. Eng., AIJ*, **75**(657), 2027-2035. https://doi.org/10.3130/aijs.75.2027.

Li, K.N., Aoyama, H. and Otani, S. (1988), "Reinforced concrete columns under varying axial load and bi-directional lateral load reversals", *Proceedings of 9th World Conference on Earthquake Engineering*, Tokyo-Kyoto, Japan, August.

Macgregor, J.G. (1988), *Reinforced Concrete Mechanics and Design*, Prentice Hall, Englewood Cliffs, N.J., USA.

Nogami, Y., Murono, Y. and Morikawa, H. (2012), "Nonlinear hysteresis model taking into account s-shaped hysteresis loop and its standard parameters", *Proceedings of 15th WCEE*, Lisbon, Portugal, September.

NZS 3101 (2006), Concrete Structures Standard, Part 1 and 2, Code and Commentary on the Design of Concrete Structures, New Zealand Standard, New Zealand.

Paulay, T., Park, R. and Priestley, M.J.N. (1978), "Reinforced concrete beam-column joints under seismic actions", *ACI Struct. J.*, **75**(11), 585–593. https://doi.org/10.14359/2856.

Shiohara, H. (2001), "New model for shear failure of RC interior beam-column connections", *J. Struct. Eng.*, **127**(2), 152-160. https://doi.org/10.1061/(ASCE)0733-9445(2001)127:2(152).

Shiohara, H. (2004), "Quadruple flexural resistance in R/C beam-column joints", *Proceedings of 13th WCEE*, Vancouver, B.C., Canada, August.

Shiohara, H. (2014), "Simplified equations predicting ultimate strength of RC beam column joints failed in joint hinging mechanism", *Summaries of Technical Papers of Annual Meeting (AIJ)*, Kobe, September.

Shiohara, H. and Kusuhara, F. (2012), "Joint shear? or column-to-beam strength ratio? which is a key parameter for seismic design of RC beam-column joints-test series on interior joints", *Proceedings of 15th WCEE*, Lisbon, Portugal, September.

Shiohara, H., Kusuhara, F. and Fujiwara, K. (2010), "Experimental study on effects of design parameters on seismic performance of exterior R/C beam-column joints", *Summaries of Technical Papers of Annual Meeting (AIJ)*, Toyama, Japan, September.

Sung, C.C. (2014), "Effects of joint aspect ratio on required transverse reinforcement of exterior joints subjected to cyclic loading", *Earthq. Struct.*, **7**(5), 705-718. https://doi.org/10.12989/eas.2014.7.5.705.

Tran, C. and Li, B. (2018), "Seismic performance of RC short columns with light transverse reinforcement", *Struct. Eng. Mech.*, **67**(1), 93-104. http://doi.org/10.12989/sem.2018.67.1.093.

Uma, S.R. and Jain, S.K. (2006), "Seismic design of beam-column joints in RC moment resisting frames-review of codes", *Struct. Eng. Mech.*, **23**(5), 579-597. http://doi.org/10.12989/sem.2006.23.5.579.

Yoshimura, M., Takaine, Y. and Nakamura, T. (2004), "Axial collapse of reinforced concrete columns", *Proceedings of 13th WCEE*, Vancouver, B.C., Canada, August.

*CC*